Homogeneous viscous flow behavior of a Cu–Zr based bulk metallic glass composites

X.Y. Zhang, Z.Z. Yuan *, X.L. Feng, L.Z. Cui, D.X. Li

State Key Laboratory of Advanced Processing and Recycling of Non-ferrous Metals, Lanzhou University of Technology, Lanzhou, Gansu 730050, China

ABSTRACT

In this paper, $Cu_{40}Zr_{44}Ag_8Al_8$ bulk metallic glass composites (BMGCs) consisting of various volume fraction of nanocrystals embedded in the amorphous matrix was synthesized by controlled annealing treatment of an as-cast BMGCs. The high temperature compression behaviors of the BMGCs were characterized in the supercooled liquid region. Results show that the flow stresses keep increasing after an initial decrease with extension of the annealing time. With annealing the values of activation volume V_{act} is determined to be increasing from 283.6216 $Å^3$ to 305.553 $Å^3$, suggesting that the jump of atoms is a cooperative process during the high-temperature deformation. Flow behavior of the BMGCs annealed for less than 8 min transform from Newtonian to non-Newtonian dependant on the stain rate and can be successively fitted by the visco-plasticity model. Fitting results indicate that deformation behaviors of these samples are governed by homogeneous flow of the amorphous matrix and indeed determined by the viscosities in the Newtonian flow stage. However, the BMGCs annealed for 8 min exhibit a non-Newtonian flow over the entire compression process and fail to be fitted by the visco-plasticity model. Micrographs of the sample reflect an impinged structure, indicating that high temperature deformation behavior of the BMGCs with high volume fractions of particles is indeed controlled by that of a backbone of particles.

© 2014 Published by Elsevier B.V.

1. Introduction

Compared with the traditional alloys, bulk metallic glasses (BMGs) have been paid worldwide attentions due to their prominent mechanical properties, including high compressive fracture strength ($\sim$2 GPa), large elastic strain ($\sim$2%), high tensile strength ($\sim$6 GPa), excellent corrosion resistance and good soft magnetic property [1–3]. Furthermore, the presence of a large supercooled liquid region (SLR) and a high thermal stability provides new opportunities for high temperature forming. Previous studies have shown that BMGs exhibit superplastic behavior in the SLR. The homogeneous flow behavior of BMGs at high temperature transit from Newtonian to non-Newtonian, depending on testing stain rate and temperature. Moreover, it is shown that the homogeneous flow behavior of BMGs can be quantitatively described by the transition state theory [4,5].

However, seldom experimental results about the homogeneous flow behavior of BMGCs have been presented up to now, keeping in mind that it is the BMGCs consisting of secondary particles in the amorphous matrix always exhibit improved properties at room temperature [6,7]. In the previous investigations, Fu et al. [8] found that rheological behavior of the Zr–Cu–Al BMGCs with various crystal volume fractions (v_f=0–20%) can be explained in terms of the transition state theory, in which Newtonian behavior followed by a transition to non-Newtonian behavior. However, in the experiments of Wang et al. [9], the partially crystallized BMGCs Vit 1 just only reveals non-Newtonian flow and the stress–strain rate relation obeys the $\sin h$ law, even though the crystal volume fractions is only 10%. The exact deformation mechanism of BMGCs is still unclear.

In the present study, compression tests will be carried out to present the high temperature deformation behavior of partially crystallized $Cu_{40}Zr_{44}Ag_8Al_8$ BMGCs and more precisely to discuss the influence of the crystals on high temperature flow behavior of the BMGCs. Deformation behavior of four different volume fractions of in situ particles are compared and a visco-plasticity model based on free volume theory was applied to explain the cause of the influence.

2. Experimental

Master ingots with a nominal composition of $Cu_{40}Zr_{44}Ag_8Al_8$ (in atomic percentage) were prepared by arc melting of pure

---

metals (99.999% purity) for 3 times in a high purity argon atmosphere, followed by suction casting into a water-cooled Cu mold to get rods with a diameter of 6 mm and length of 30 mm under 7 kW of power and negative pressure of 0.02 MPa by the electro magnetic levitation suction casting equipment. The investigated BMGCs with various volume fractions of nanocrystals dispersed in the amorphous matrix were synthesized by isothermally annealing the as-cast samples at the temperature of 738 K in the supercooled liquid region for different times (0, 3, 5, 8 min).

The thermal characteristic parameters of the BMGCs were determined by differential scanning calorimeter (DSC, NETZSCH STA 449C Instruments) at the heating rate of 20 K min^{-1}. T_g was determined to be 706 K for the sample, whereas T_x was 784 K. The thermal parameters are comparable to those studied by Liu et al. Hence the sample exhibits a large SCL region up to 78 K. The microstructure of the BMGCs were investigated by X-ray diffractometer (XRD, Japan Nikkaku D/max-2400, Cu K_α) and scanning electron microscopy (SEM, JSM-6700F). The etched solutions were 1% hydrofluoric acid aqueous solution for SEM observation.

To minimize the experimental errors for various strain rates between different experimental conditions and samples, strain rate jump compression tests were carried out. For compression tests, cylindrical samples with an aspect ratio of 1:2 were cut from the rods by a diamond slicing machine and both compressive sides were polished in order to be parallel. High temperature compression tests were conducted using a Gleeble 3500 machine at $T_a = 721$ K in the SCL region. Thermocouples were welded in the middle of the samples to detect in situ the test temperature. To minimize or avoid crystallization during the heating stage, the tests should be conducted as soon as possible. First heat the samples quickly to $T_a - 40$ K at the rate of 10 K s^{-1}. Then heat them to T_a at the same rate of 20 K min^{-1} as used in DSC measurements, considering the fact that T_g is not a unique physical property of the glass but rather a rate dependent kinetic quantity. Compression testing started only after the samples were maintained at T_a for 30 s to homogenize temperature. The investigated true strain rate interval was from 2.5×10^{-4} to 1×10^{-2} s^{-1}.

3. Results and discussion

3.1. Materials characterization

Fig. 1 shows XRD pattern of the as-cast $Cu_{40}Zr_{44}Ag_8Al_8$ sample. The XRD pattern showed a broad halo peak, characteristic of the amorphous phase. Fig. 2 shows SEM observation of the BMGCs isothermally annealed at 738 K fo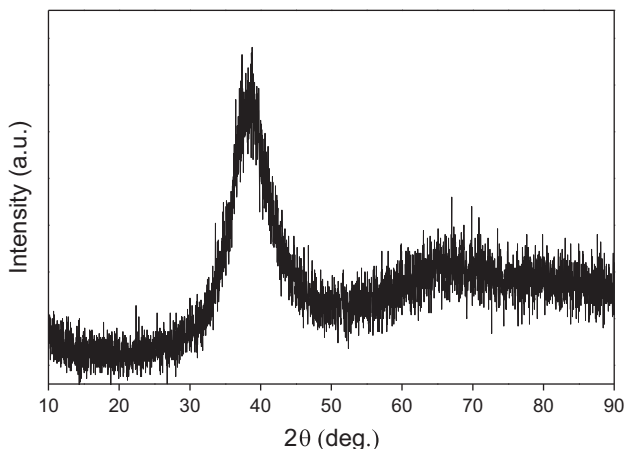r 0, 3, 5, 8 min. SEM image of the as-cast sample reveals a few nano-sized precipitates in the range of 20–50 nm embedded in the amorphous matrix, as shown in Fig. 2(a). In contrast, SEM images of the other three annealed samples show that particles with a spherical size about 500 nm have precipitated from the amorphous matrix, as shown in Fig. 2 (b)–(d). Especially for the sample annealed for 8 min, particles precipitate from the amorphous matrix in a large number and start to impinge to each other.

3.2. Deformation behavior of the as-cast samples

In order to determine the rheology information of the BMGCs, strain rate jump tests were carried out at the temperature of 721 K and the Backofen function is introduced [10].

$$\sigma_{flow} = K\dot{\varepsilon}^m \tag{1}$$

where σ_{flow} is the flow stress, K is a constant, $\dot{\varepsilon}$ is the strain rate and m is the strain rate sensitivity exponent.

Taking the logarithm leads to the relationship

$$\lg \sigma = m \lg \dot{\varepsilon} + \lg K \tag{2}$$

a straight line, whose slope yields the value m.

According to Refs. [10,11], the flow stress is defined as the peak-yield stress in order to minimize the elastic contribution (the elastic strain rate $\dot{\sigma}/E = 0$ at the peak stress). Thus to ensure that the stresses can reach to the peak-yield points and the measurements are performed within the shortest time in order to avoid structural modification taken place in the amorphous matrix, a strain interval of 0.04 is chosen for each strain rate. In the compressive process, drum shape is formed on the side surface of the cylindrical billet, which is similar to the upsetting process of the alloy [12]. The photograph of the deformed sample is shown in the inset of Fig. 3. The sample keeps a smooth surface without any cracks until the tested strain reached $\varepsilon = 36\%$, indicating the BMGCs process a homogenous flow behavior during high temperature deformation.

Fig. 3 shows true stress versus true strain curve of the as-cast samples obtained by strain rate jump compression test performed at 721 K. It is noted that even at the highest strain rates the material still exhibits fully homogenous deformation behavior, which indicates a good compressibility of the BMGCs. The steady state plastic flow was observed at low strain rate. However, when the testing strain rate is increased (e.g. $\dot{\varepsilon} = 2.5 \times 10^{-4}$ s^{-1}), stress overshoots are observed whose amplitude is obviously increasing with the strain-rate, as had been extensively studied [13,14].

3.3. Viscosity flow behavior of all the BMGCs

Fig. 4 shows stress–strain curves of all the BMGCs. Deformation curves of the annealed samples are quite similar to that of the as-cast sample, which is seriously dependent on the testing strain rate. As the strain rate increasing, steady state plastic flow changes to obvious stress overshoots. Furthermore, it is remarkable to note that the flow stresses keep increasing after an initial decrease with extension of the annealing time.

According to Kim [15], due to the differences in the thermal and elastic properties between particles and amorphous matrix, residual stress can arise during the sample preparation. He demonstrated the higher compressive strength in W-rich particle-reinforced Ti-based BMGCs as being the result of the generation of tensile residual stress in the amorphous matrix upon cooling during sample preparation. In the case of ceramic particle-reinforced alloy composites [16], it has been explained that it is also the tensile residual stress that contribute to the high compressive strength. A similar effect is expected to work in the as-cast $Cu_{40}Zr_{44}Ag_8Al_8$ BMGCs. Residual stress would normally be left

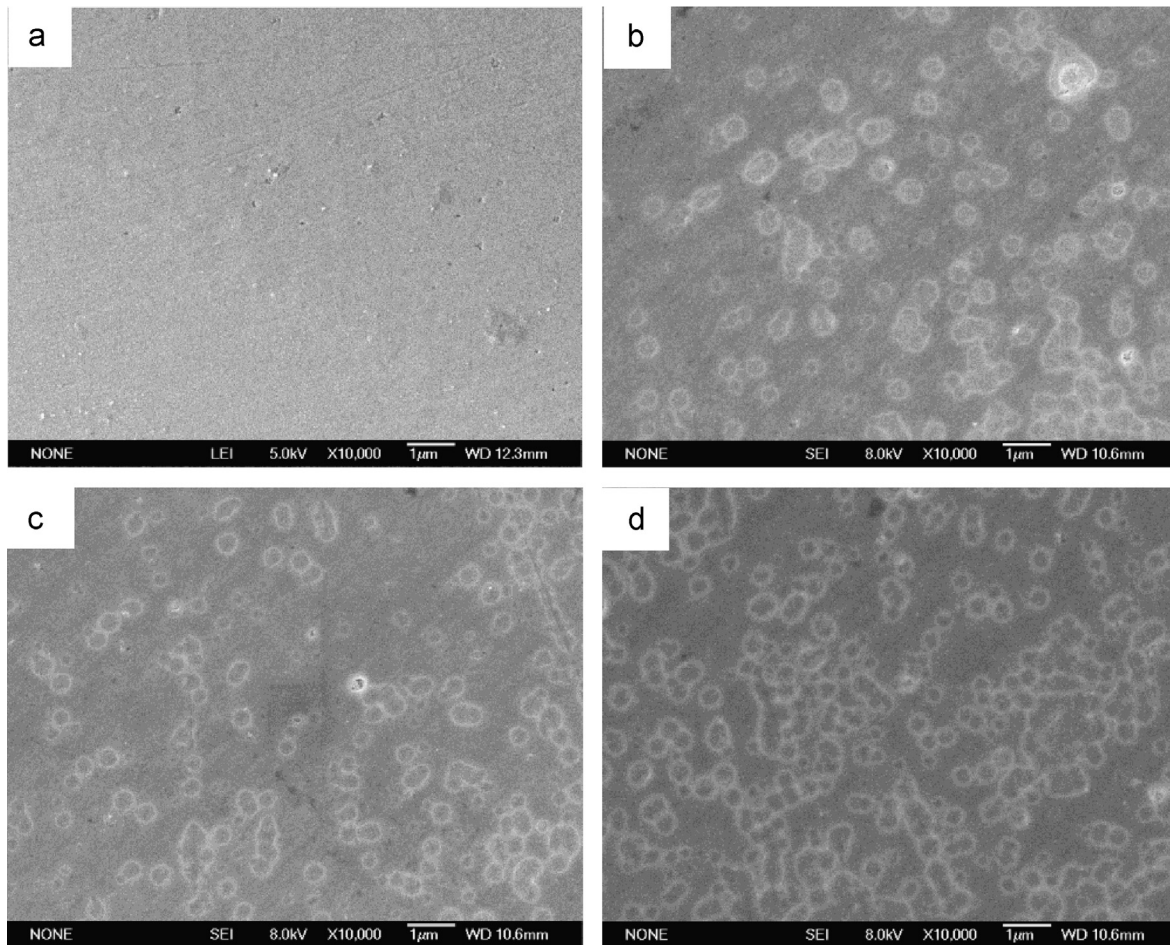**Fig. 1.** XRD pattern of the as-cast $Cu_{40}Zr_{44}Ag_8Al_8$ sample.

Fig. 2. SEM observations of the BMGCs isothermally annealed at 738 K for (a) 0, (b) 3, (c) 5, and (d) 8 min.
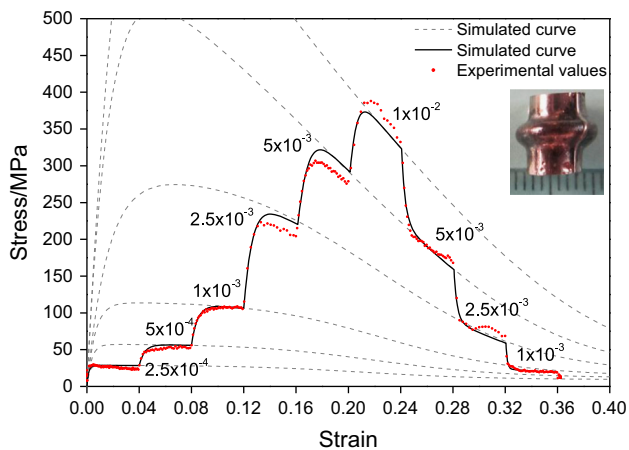

Fig. 3. Stress–strain curves for the as-cast sample at 721 K with the photograph of the deformed sample shown in the inset. The strain-rate jumps range from 2.5×10^{-4} up to 1×10^{-2} s^{-1} and down again to 1×10^{-3} s^{-1}.

Fig. 4. Typical stress–strain curves obtained by strain rate increase tests on Cu$_{40}$Zr$_{44}$Ag$_8$Al$_8$ BMGCs performed at 721 K.

in the BMGCs upon cooling due to the difference in the coefficients of thermal expansion between the particles and the amorphous matrix, which give rise to the high compressive strength of the as-cast sample.

With the structural relaxation takes into effect during annealing and heating process, residual stresses are diminished or vanished, which leads to a decreased yield stress. Therefore, strength of the annealed samples has a downward trend after annealing for 3 min, even though the nano-particles have start to
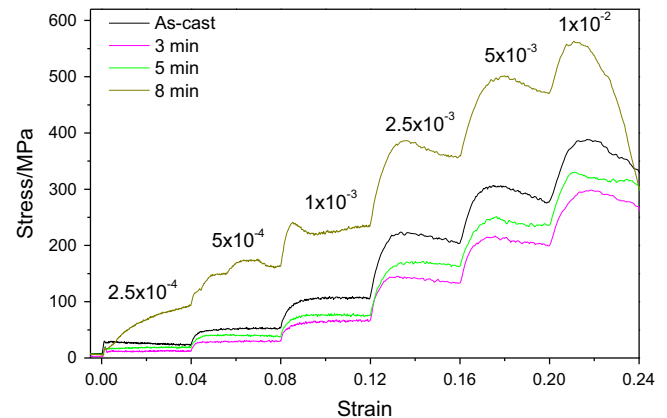
precipitate from the amorphous matrix. However, continued annealing leads to an increased volume fraction of grain nucleation and growth and eventually results in the rise of the compressive strength. The strengthening mechanisms of precipitates have been explained by two contributions for other Zr-based BMGCs [8]: (i) load transfer from the glass to the particles; and (ii) shift of the glass structure and properties. Especially for the sample annealed for 8 min, annealing not only increase the strength of the BMGCs quickly, but also extend the stress overshoot phenomenon to all the strain rates.
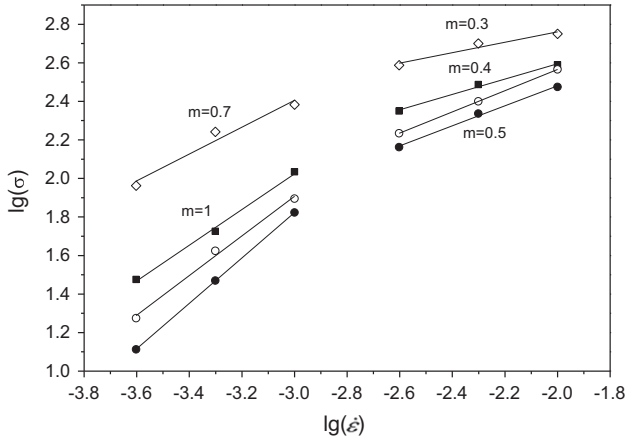
Fig. 5. Logarithm stresses versus logarithm strain rates and m values of the BMGCs deformed at 721 K.

Fig. 6. Strain rate as a function of strength derived from the strain rate jump compression test.

Using experimental data from Fig. 4, the double logarithmic plots of stress as a function of strain rate were performed. Fig. 5 compares the stress–strain rate relationship of all the BMGCs. It is noted that the BMGCs annealed for less than 8 min display a clear transformation from Newtonian to non-Newtonian in flow behavior. When the strain rates are no more than $1 \times 10^{-3}\,\mathrm{s}^{-1}$, the BMGCs display a homogeneous Newtonian flow with the value of m is close to unity. As the strain rate increases, the m value decreases to no more than 0.5, suggesting that the BMGCs has transformed to non-Newtonian fluid body. This transition has been argued by Nieh [17] as a general phenomenon for superplastic deformation of amorphous alloy. In a word, annealing does not change flow behaviors of the BMGCs when the annealing time is less than 8 min.

However, the BMGCs annealed for 8 min exhibit a non-Newtonian flow over the entire compression process, indicating that crystal volume fraction significantly affect flow behavior of the BMGCs. The BMGCs transform to non-Newtonian flow when the crystal volume fraction is increased to a certain point by annealing.

According to Spaepen [18], the relationship between applied strain-rate ($\dot{\varepsilon}$) and stress (σ) in uniaxial steady-state deformation can be given as follows:
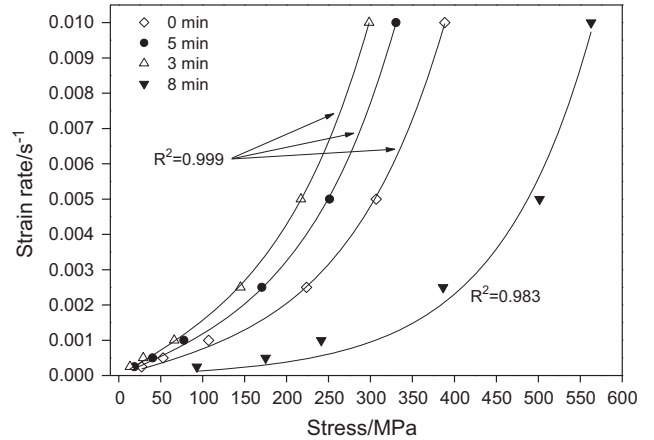
$$\dot{\varepsilon} = \dot{\varepsilon}_0 \sinh\left(\frac{\sigma V_{act}}{2\sqrt{3}KT}\right) \tag{3}$$

where V_{act} ($=\varepsilon_0 v_0$, v_0 is the volume of a flow unit which undergoes a strain ε_0 during deformation, $\varepsilon_0 < 1$, which depends on temperature and material) is the activation volume, kT has its usual meaning, and $\dot{\varepsilon}_0$ captures the amplitude of temperature dependence on flow:

$$\dot{\varepsilon}_0 = c_f \dot{\varepsilon}_{0,T} = ac_f v_G \exp\left(-\frac{\Delta F}{RT}\right) \tag{4}$$

where $a = a_0 c_f$ (≈ 1 for homogeneous flow), a_0 is a numerical factor, c_f is the defect concentration derived from the free volume. v_G is the normal mode frequency of the flow unit STZ along the activation path, ΔF is the Helmholtz free energy barrier or activation energy, and $\dot{\varepsilon}_{0,T}$ the frequency factor, which is constant at a given temperature.

Since all of the experiments were conducted at the same temperature, it is not required to take into account the temperature-dependent details in Eq. (4). Fig. 6 shows the strain rate dependence of the flow strength which can be quantitatively derived by fitting Eq. (3) to the experimental data. It is clear that the stress–strain curves had almost the same shapes and all of

them follow the transition state theory, suggesting that the deformation behaviors of all the BMGCs may be dominated by the homogeneous flow of the amorphous matrix phase. However, it is interesting to note that the coefficient of determination R^2 reduces to 0.983 from 0.999, indicating that flow behavior of the BMGCs annealed for 8 min have begun to deviate from the transition state theory.

The fitting results are given in Table 1. In Eq. (3), $\dot{\varepsilon}_0$ affects the position of the curve, while V_{act} influences the curvature of the data. The variations in $\dot{\varepsilon}_0$ opposite to changes in peak stress for various samples. The values of activation volume V_{act} are slightly increasing with annealing and of the same order as the previously reported data for BMGs, e.g. $V_{act} = 150$–200 Å^3 for Zr$_{52.5}$Al$_{10}$Cu$_{27}$Ti$_{2.5}$Ni$_8$ BMGs [19], $V_{act} = 280$–380 Å^3 for Mg$_{65}$Cu$_2$Gd$_{10}$ BMGs [20], $V_{act} = 215$–300 Å^3 for Ti$_{41.5}$Cu$_{37.5}$Ni$_{7.5}$Zr$_{2.5}$Hf$_5$Sn$_5$Si$_1$ BMGs [5] and $V_{act} = 162$–167 Å^3 for Cu$_{47.5}$Zr$_{47.5}$Al$_5$ BMGs [21]. Providing the average atomic volume of the alloy is about 10.636 Å^3, a unit local flow event at least includes 27–29 atoms for the BMGCs during the high-temperature deformation. The results suggest that the jump of atoms is a cooperative process during the high-temperature deformation. Specially, shear transformation zones (STZs) of the BMGCs annealed for less than 8 min contain about the same atoms. But STZs of the samples annealed for 8 min takes more atoms into action, indicating that STZs of the more ordered structures involve more atoms. Chen et al. also found that the V_{act} for the (Zr$_{75}$Cu$_{25}$)$_{74.5}$Ta$_8$Ni$_{10}$Al$_{7.5}$ BMGCs is much higher than that of the corresponding BMGs [22]. On the contrary, Fu et al. [8] have presented that V_{act} is reasonably constant with composition for Zr–Cu–Al BMGCs with various volume fractions of particles. This is because the changes in crystal volume fraction caused by the composition difference are too small to affect the STZs size. The same phenomenon can also be seen in our experiment for the samples annealed for less than 8 min.

Table 1
Fitting parameters used in Eq. (3) for the BMGCs and fully amorphous alloy at 723 K.

Parameters	0 min	3 min	5 min	8 min
V_{act} (Å^3)	283.6216	287.735	290.134	305.553
Atoms	27	27	27	29
$\dot{\varepsilon}_0 Z(\mathrm{s}^{-1})$	8.24×10^{-4}	1.679×10^{-3}	1.253×10^{-3}	1.34×10^{-4}

3.4. Viscosity analysis

For ideal Newtonian viscous flow, both shear stress, τ, and shear strain rate, $\dot{\gamma}$, have a linear relationship under the uniaxial deformation, i.e. $\tau = \eta\dot{\gamma}$. Combing strain rate in Eq. (3), one obtains the non-Newtonian viscosity η (effective stress, $\sigma = \sqrt{3}\tau$, and effective strain rate, $\varepsilon = \dot{\gamma}/\sqrt{3}$):

$$\eta = \frac{\tau}{\dot{\gamma}} = \frac{\tau}{\dot{\gamma}_0 \sinh{(\tau V_{act}/2kT)}} = \frac{\sigma}{3\dot{\varepsilon}_0 \sinh{(\sigma V_{act}/2kT)}} \quad (5)$$

Fig. 7 shows the variation of the viscosity with strain rate. The dependence of η on strain rate is well known as shear thinning behavior which is a character of BMGs. For low strain rates, the viscosity of the BMGCs annealed for less than 8 min is nearly independent of strain rate, indicating a Newtonian behavior. The flow behavior confirmed by η agrees with the results gained by m.

If the flow defect concentration is assumed to maintain at the equilibrium and $V_{act} \ll kT$, the Newtonian viscosity is then can be rewritten as

$$\eta_N = \frac{2kT}{\sqrt{3}\dot{\varepsilon}_0 V_{act}} \quad (6)$$

A normalized viscosity can be written as

$$\frac{\eta}{\eta_N} = \frac{x}{\sinh{(x)}} \quad (7)$$

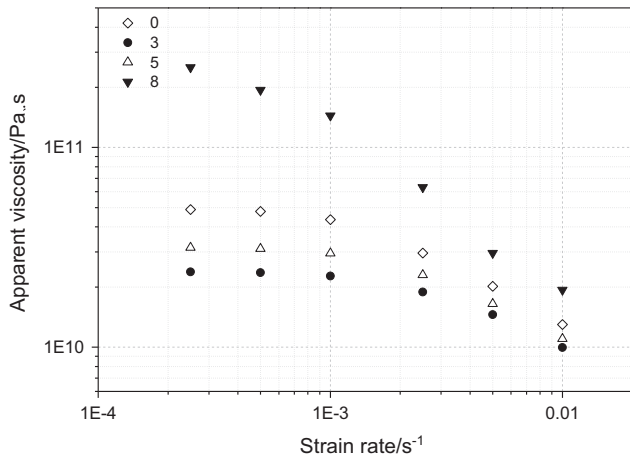with $x = \dfrac{\sigma V_{act}}{2\sqrt{3}kT}$

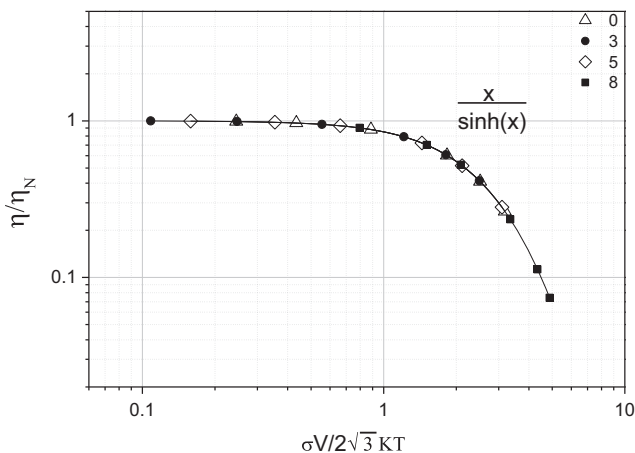**Fig. 7.** The apparent viscosity of the BMGCs annealed for different times.

Fig. 8. Master curve of normalized viscosity derived from Eq. (7).

Fig. 8 shows the variation of η/η_N obtained at various strain rates for all the $Cu_{40}Zr_{44}Ag_8Al_8$ BMGCs fall on this master curve. This agreement supports the hypothesis that the defect concentration is roughly constant in the investigated domain for the samples and flow behavior of the BMGCs seems to still be dominated by the amorphous matrix.

3.5. Deformation constitutive equations

In fact, the strain rate in Eq. (3) corresponds only to plastic deformation. According to Bletry [23], to simulate the high temperature deformation behavior of the amorphous alloy, the strain rate has to be coupled with the elastic and inelastic strain rate

$$\dot{\varepsilon} = c_f\dot{\varepsilon}_{0,T} \sin{h\left(\frac{\sigma V}{2\sqrt{3}kT}\right)} + \frac{\dot{\sigma}}{E} + \frac{\sigma}{\eta_a} \quad (8)$$

where E and η_a are the Young's modulus and the inelastic modulus during high temperature deformation at temperature T, respectively. This visco-plasticity model is able to describe the appearance of a stress overshoot when the strain-rate increases, and even the appearance of a stress oscillation. In the experiments of Bletry et al. [24], mechanical behavior of partially crystallized BMGCs was precisely simulated by introducing the "backstress" model [25] which was proposed to solve strain hardening resulting form unrelaxed plastic incapability in composite materials. However, backstress effect can be neglected in our experiment domain for $Cu_{40}Zr_{44}Ag_8Al_8$ BMGCs due to the fact that our previous analysis has revealed that flow behaviors of the BMGCs are mainly dominated by the amorphous matrix and strain hardening phenomenon has not be seen in our experiment, as shown in Fig. 4.

It is noted that the previous estimation was operated under the hypothesis that defect concentration c_f is constant in steady state condition. However, homogeneous flow at the high strain rates in our experiments is obviously occur under non-steady state conditions where stress overshoots caused by excessive free volume were revealed on the stress–strain curve. In this case, c_f is a competition between the creation and annihilation of flow defects induced by plastic strain and structural relaxation, respectively. Such a framework has been considered by de Hey et al. [26], where the flow concentration is given by

$$\dot{c}_f = a_x\dot{\varepsilon}c_f\ln^2 c_f - k_r c_f(c_f - c_{f,eq}) \quad (9)$$

where a_x is the creation factor, in proportion to temperature as $a_x = 3kT(1\text{-}\nu)/\xi\nu^*G(1+\nu)$ with ν the Poisson ratio and G the shear modulus. K_r is temperature-dependent rate constant of the structural relaxation, which is thermally activated. $c_{f,eq}$ is the equilibrium of defect concentration, which can be described by the Arrhenius law: $c_{f,eq} = c_0\exp(-\Delta G^f/kT)$, where ΔG^f is the formation free energy of the flow defects. The first term in Eq. (9) corresponds to the defects creation by plastic deformation whereas the second term represents the static thermal annihilation and creation of defects. In this framework, the steady state homogeneous flow condition in the previous assumption corresponds to the situation of $\dot{c}_f = 0$ and c_f is essentially a constant due to the balance between free volume creation and annihilation.

Numerical solving of Eqs. (8) and (9) allows simulation of the high temperature deformation of BMGs in a given domain. With V_{act} values listed in Table 1 and the initial flow defect concentration $c_{f,i}(c_{f,i} = 2.5 \times c_{f,eq})$, the parameters in the simultaneous equations can be determined uniquely by fitting the predicted curves to the experimental data. Since stress is independence of the stress–strain path history, typical stress–strain curves of constant strain rate and strain rate jump tests for the as-cast sample are reported in Fig. 3. A relatively good agreement is acquired between the prediction and the experiment; in particular, the strain rate
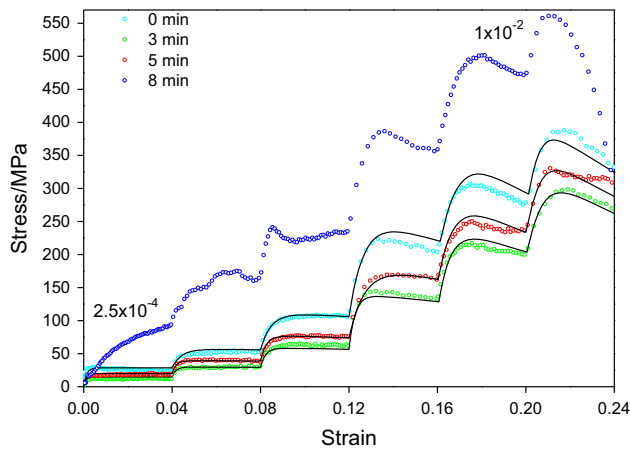
Fig. 9. Comparison between experiment (points) and model (line) for the strain-rate jumps experiments at 721 K.

Table 2
Fitting parameters for Superplastic deformation of all the BMGCs at 721 K.

Sample	a_x	k_r	$c_{f,eq}$	$\varepsilon_{0,T}$	η_α	$\bar{\eta}$	$\eta_\alpha/\bar{\eta}$
0 min	0.035	3×10^7	1×10^{-13}	1.5×10^7	1.15×10^{11}	4.6×10^{10}	2.5
3 min			1.5×10^{-13}		6×10^{10}	2.4×10^{10}	2.5
5 min			1.5×10^{-13}		8×10^{10}	3.2×10^{10}	2.5

decrease experiment and the variation in stress overshoot amplitude with relaxation time.

Fig. 9 compares the experimental data with the predicted curves of the strain rate jump tests for all the BMGCs. With the parameters shown in Table 2, the model fits well on the experimental data and the predicted curves except for the sample annealed for 8 min, indicating high temperature deformation behavior of the BMGCs with high volume fractions of particles cannot be described by the visco-plasticity model. In fact, the micrographs reflect an impinged structure in the sample annealed for 8 min. Thus it is reasonable that backbone of particles could prevent the amorphous matrix from freely flow during compression. It is in line with Fu's [27] discovery that creep of the Zr-based BMGCs is indeed controlled by that of a percolating dendritic structure of La when the dendrite network formed.

It is to be noted that the parameters a_x, k_r and $\varepsilon_{0,T}$ are constant for the samples annealed less than 8 min, which is consistent with the definition of these parameters at a given temperature. The parameter $c_{f,eq}$ depends only on temperature and can be qualified as a constant for BMGs at a given temperature. But in our experiment, the term increases from 1×10^{-13} to 1.5×10^{-13}. The slight variation of $c_{f,eq}$ may be caused by the microstructure evolution of the BMGCs with various crystal volume fractions. However, the parameters η_α change in the range from 6×10^{10} to 1.15×10^{11} poise. The results show that the variation of η_α is quite similar to the variation of the stress of the BMGCs during compression, suggesting that flow behavior of the BMGCs annealed less than 8 min is indeed determined by the parameter η_α.

Although the visco-plasticity model was proposed by Bletry et al. [28] to rationalize the stress overshoot phenomenon and was proved to be suitable for superplastic flow behavior of certain BMGs, they failed to give a physical meaning to the parameter η_α due to the ultra low apparent value of the Young's modulus. But in our experiment, the true stress-stain curves of the strain rate jump compression test for all the samples annealed less than 8 min are successfully fitted with the E values measured from the experimental curves. Furthermore, the parameter η_α in the fitting results is actually in direct proportion to the average apparent viscosity $\bar{\eta}$

in the Newtonian flow stage for all the BMGCs: $h = \eta_\alpha/\bar{\eta} = 2.5$, as shown in Table 2. Consequently, the strain rate at a temperature T can be written in the form

$$\dot{\varepsilon} = c_f \dot{\varepsilon}_{0,c} \sinh\left(\frac{\sigma V}{2\sqrt{3}kT}\right) + \frac{\dot{\sigma}}{E} + b\frac{\sigma}{\eta_a} \tag{10}$$

where $b = 1/h$, the inelastic factor giving the proportionality between inelastic strain rate and the total stain rate. In the present study, a value $b = 0.4$ is obtained from fitting. But this term is approximately 0.1 for the $Zr_{52.5}Al_{10}Cu_{22}Ti_{2.5}Ni_{13}$ BMGs in reference [19], which may be caused by the relative high deformation temperature and low viscosity effect. Therefore, the parameter η_α is equal to the true viscosity in Newtonian flow stage and has its physical meaning as viscosity, at least for the Newtonian flow stage.

4. Conclusions

The homogeneous deformation behaviors of a series of $Cu_{40}Zr_{44}Ag_8Al_8$ BMGCs with various crystal volume fractions of particles have been studied. The salient findings are as follows:

1. The true stress–strain curves of high temperature compression prove that the flow stresses keep increasing after an initial decrease with extension of the annealing time.
2. Stress–strain rate relationship reveals that flow behavior of the BMGCs annealed for less than 8 min transform from Newtonian to non-Newtonian with increase of the strain rate. However, the BMGCs annealed for 8 min exhibit a non-Newtonian flow over the entire compression process.
3. Deformation behaviors of the samples annealed for less than 8 min are governed by homogeneous flow of the amorphous matrix and all of them follow the transition state theory. But the coefficient of determination indicates that flow behavior of the BMGCs annealed for 8 min have begun to deviate from the transition state theory. The fitting results reflect that the values of activation volume V_{act} is increasing from 283.6216 Å^3 to 305.553 Å^3 with annealing, suggesting that the jump of atoms is a cooperative process during the high-temperature deformation.
4. True stress–strain curves of the samples annealed for less than 8 min can be successively fitted by the visco-plasticity model. Fitting results indicate that the flow behavior of the BMGCs annealed less than 8 min is indeed determined by viscosity in the Newtonian flow stage. But the visco-plasticity model failed to fit the true stress–strain curves of the samples annealed for less than 8 min. Micrographs of the sample reflect an impinged structure, indicating that high temperature deformation behavior of the BMGCs with high volume fractions of particles did not follow the visco-plasticity model and is indeed controlled by that of a backbone of particles.

References

[1] C. Fan, R.T. Ott, T.C. Hufnagel, Appl. Phys. Lett. 81 (2002) 1020.
[2] C.Y. Haein, S.Y. Lee, D.C. Robert, Scr. Mater. 58 (2008) 763.
[3] Y. Liu, J.J. Blandin, G. Kapelski, M. Suéry, Mater. Sci. Eng. A 528 (2011) 3748.
[4] L. Liu, Q. Chen, K.C. Chan, J.F. Wang, G.K.H. Pang, Mater. Sci. Eng. A 449–451 (2007) 949.

[5] J.N. Mei, J.L. Soubeyroux, J.J. Blandin, J.S. Li, H.C. Kou, H.Z. Fu, L. Zhou, Intermetallics 19 (2011) 48.
[6] C. Li, J.S.C. Jang, J.B. Li, D.J. Pan, S.R. Jian, J.C. Huang, T.G. Nieh, Intermetallics 30 (2012) 111.
[7] J.S.C. Jang, T.H. Li, S.R. Jian, J.C. Huang, T.G. Nieh, Intermetallics 19 (2011) 738.
[8] X.L. Fu, Y. Li, C.A. Schuh, Acta Mater. 55 (2007) 3059.
[9] Q. Wang, J.J. Blandin, M. Suery, B. Van de Moortéle, J.M. Pelletier, J. Mater. Sci. Technol. 19 (2003) 557.
[10] W.J. Kim, D.S. Ma, H.G. Jeong, Scr. Mater 49 (2003) 1067.
[11] T.G. Nieh, J. Wadsworth, C.T. Liu, T. Ohkubo, Y. Hirotsu, Acta Mater. 49 (2001) 2887.
[12] Y.C. Lin, M.S. Chen, J. Zhong, Comput. Mater. Sci. 43 (2008) 1117.
[13] Y. Kawamura, T. Shibata, A. Inoue, T. Masumoto, Mater. Trans. JIM 40 (1999) 335.
[14] Q. Wang, D.K. Wang, T. Fu, J.J. Blandin, J.M. Pelletier, Y.D. Dong, J. Alloys Compd. 495 (2010) 50.
[15] Y.C. Kim, E. Fleury, J.C. Lee, D.H. Kim, J. Mater. Res. 20 (2005) 2474.
[16] R.J. Arsenault, M. Taya, Acta Metall. 35 (1987) 651.
[17] T.G. Nieh, J. Wadsworth, Scr. Mater. 54 (2006) 387.
[18] D. Henann, L. Anand, Acta Mater. 56 (13) (2008) 3290–3305.
[19] M. Bletry, P. Guyot, Y. Bréchet, J.J. Blandin, J.L. Soubeyroux, Acta Mater. 55 (2007) 6331.
[20] B. Gun, K.J. Laws, M. Ferry, Mater. Sci. Eng. A 471 (2007) 130.
[21] K.S. Lee, H.J. Jun, S. Pauly, B. Bartusch, Y.W. Chang, J. Eckert, Intermetallics 17 (2009) 65.
[22] Q. Chen, L. Liu, K.C. Chan, Sci. China Ser. G – Phys. Mech. Astron. 51 (2008) 349.
[23] M. Bletry, P. Guyot, J.J. Blandin, J.L. Soubeyroux, Acta Mater. 54 (2006) 1257.
[24] M. Bletry, P. Guyot, Y. Bréchet, J.J. Blandin, J.L. Soubeyroux, Intermetallics 12 (2004) 1051.
[25] L.M. Brown, D.R. Clarke, Acta Metall. 23 (1975) 821.
[26] P. de Hey, J. Sietsma, A. van den Beukel, Acta Mater. 46 (1998) 5873.
[27] X.L. Fu, Y. Li, C.A. Schuh, J. Mater. Res. 22 (2007) 1564.
[28] M. Bletry, P. Guyot, Y. Bréchet, J.J. Blandin, J.L. Soubeyroux, Mater. Sci. Eng. A 387–389 (2004) 1005.